

# **Detonation Front Models: Theories and Methods**

---

**John Bdzil**

Los Alamos National Laboratory

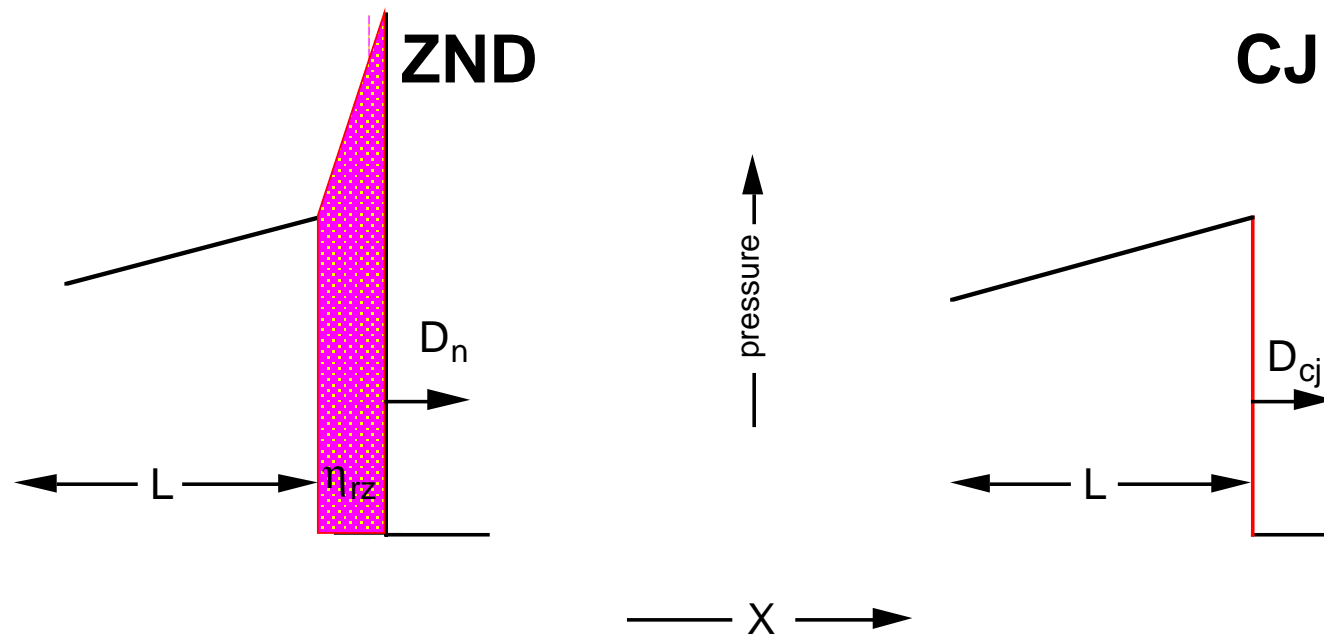
Contributors:

**Tariq Aslam (LANL), John Bdzil (LANL),  
Rudy Henninger (LANL), Ash Kapila (RPI), Scott Stewart (UIUC)**

***IMA Workshop on: High-speed Combustion in  
Gaseous and Condensed-phase Energetic Materials  
Nov 8-12, 1999***

# Detonation Propagation

- combustion supported shock wave
- shock provides energy transport and reaction ignition
- inertial confinement (shock) yields high pressures and fast chemical reactions

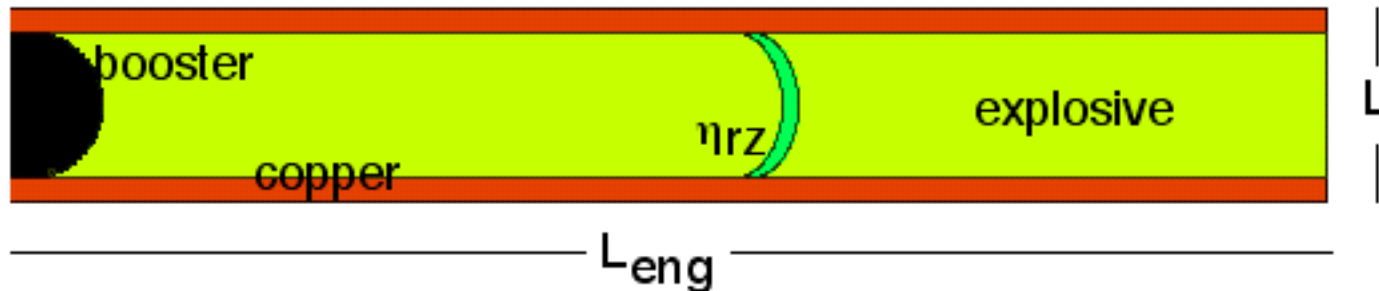


- CJ is zeroth order model

# Multi-Scale Issues - 1

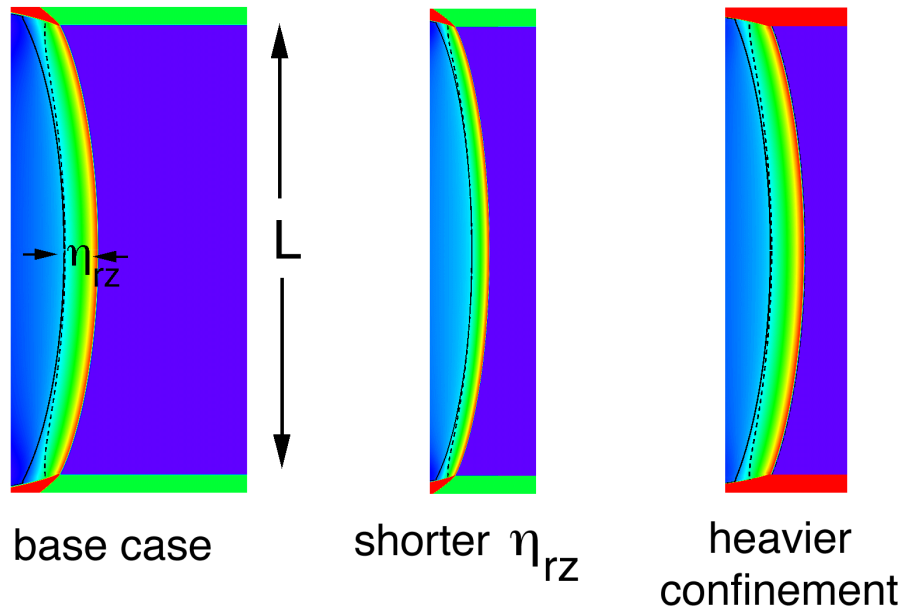
---

- consider the detonation of a cylinder of high explosive



- disparate length scales ( $L_{eng} \gg L \gg \eta_{rz}$ )
- reaction rate effects important even when  $L \gg \eta_{rz}$
- finiteness of  $\eta_{rz}/L$  influences propagation speed,  $D_0$ , and pressure of detonation through edge effects

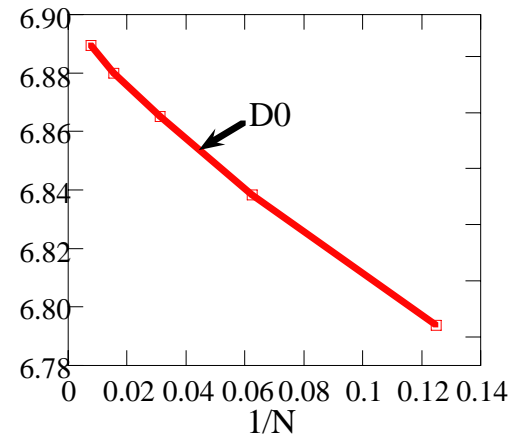
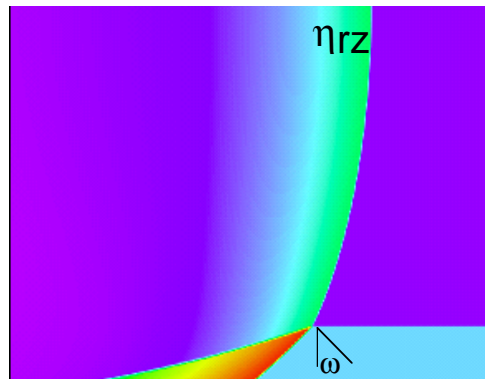
# Multi-Scale Issues - 2



- $D_0$  decreases as  $\eta_{rz}/L$  increases
- $D_0$  decreases as confinement decreases
- detonation extinction and a host of other phenomena depend on the value of  $\eta_{rz}/L$
- CJ model doesn't describe these effects

# DNS of Detonation

- given a well calibrated “reactive Euler model,” these effects can be calculated via direct numerical simulation (DNS)
- resolved DNS requires fine zoning



- O(50 pts) are needed in the reaction zone to get  $D_0$  converged to O(0.02 mm/us) using modern, hi-res methods. Multistep reaction models require more resolution. Maximum error of 1% in computed  $\eta_{rz}$

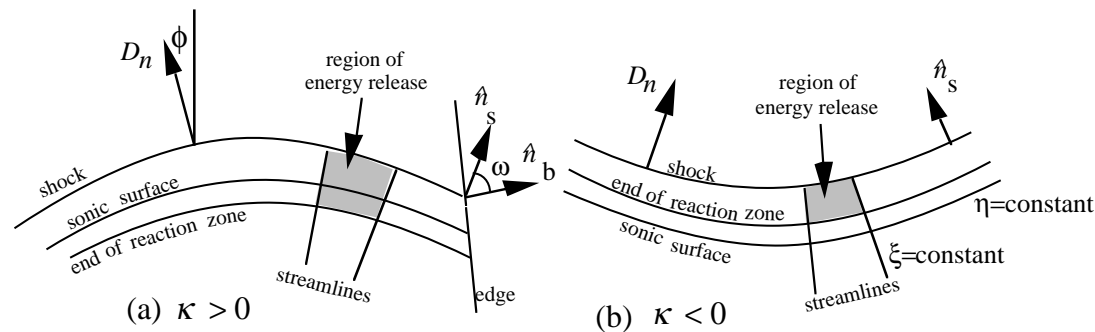
# DNS Cost Estimates

---

- instantaneous volume of 3D reaction zone,  $V_{rz}$ , is  $V_{rz} \sim (L_{eng})^2 \eta_{rz}$ . For  $L_{eng} \sim 300\text{mm}$ ,  $\eta_{rz} \sim 1\text{mm}$  and 50 points in the  $\eta_{rz}$  direction,  $O(10^{10})$  cells in the reaction zone at any instant
- with  $\Delta t = 4 \times 10^{-3} \mu\text{s}$  and a problem time of  $50 \mu\text{s}$  gives  $1.25 \times 10^4$  time steps
- grind time of  $10^{-4}$  s/cell/cycle
- computation time for the reaction zone only  
 $T_{cpu3D} \sim (10^{-4})(10^{10})(1.25 \times 10^4) = 1.45 \times 10^5$  days
- 1,000 cpu perfect parallelization,  $T_{cpu3D||} = 145$  days
- with AMR, 2D calculations may be feasible
- a subscale model of detonation propagation is indicated

# Detonation Shock Dynamics (DSD)

- detonation is supersonic combustion, insulated from the combustion products flow
- principally, detonation communicates with its surroundings laterally (sideways flow)
- the fundamental balance that sets the normal speed of detonation,  $D_n$ , is the interaction between chemical heat addition and flow divergence in the reaction zone



# DSD - 2

---

- a subscale model for the motion of the detonation front, decoupled from the post reaction zone flow
- the fundamental balance is described by the product,  $(\eta_{rZ} \kappa)$ , where  $\kappa$  is the shock curvature. Typically,  $(\eta_{rZ} \kappa) = O(\varepsilon)$ , with  $\varepsilon \ll 1$ , which defines a perturbation parameter for an asymptotic analysis

$$\frac{\partial \rho}{\partial t} + \bar{\nabla} \cdot (\rho \bar{u}) = 0,$$

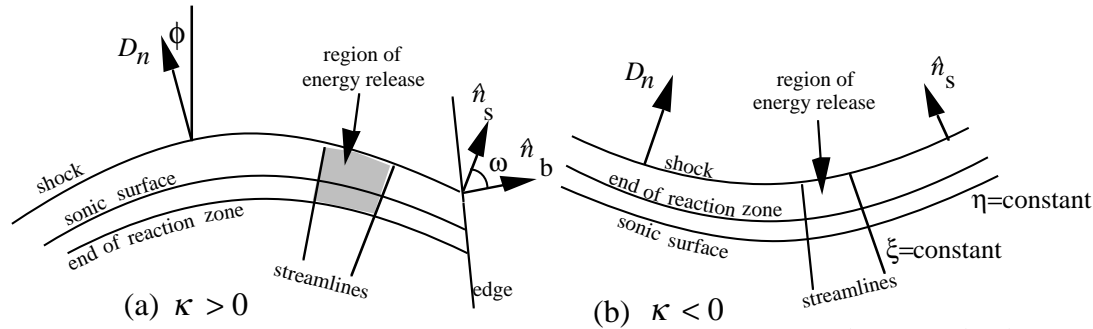
$$\frac{\partial \rho \bar{u}}{\partial t} + \bar{\nabla} \cdot (\rho \bar{u} \bar{u} + \bar{I} P) = 0,$$

$$\frac{\partial \rho e}{\partial t} + \bar{\nabla} \cdot [(\rho e + P) \bar{u}] = 0,$$

$$E(P, \rho, \lambda) = \frac{P/\rho}{\gamma - 1} - q\lambda, \quad \frac{d\lambda}{dt} \equiv R = k(1 - \lambda)^\mu \left( \frac{P}{P_{cj}} \right)^n,$$

# DSD - 3

- intrinsic (Bertrand) coordinate analysis of the reactive Euler equations rewritten in quasi-conservation form



$$[\rho(D_n - u_\eta)]_{,\lambda} = -\frac{A}{(R - \mathcal{L}(\lambda))},$$

$$[\rho(D_n - u_\eta)^2 + P]_{,\lambda} = \frac{B}{(R - \mathcal{L}(\lambda))},$$

$$\left[ E + 1/2(D_n - u_\eta)^2 + \frac{P}{\rho} \right]_{,\lambda} = \frac{C}{(R - \mathcal{L}(\lambda))},$$

$$[u_\xi]_{,\lambda} = \frac{\mathcal{E}}{(R - \mathcal{L}(\lambda))},$$

$$A = (D_n - u_\eta) \cdot (\mathcal{G} + \mathcal{L}(\rho)),$$

$$B = (D_n - u_\eta) \cdot ((u_\eta - D_n) \cdot \mathcal{G} + \rho \mathcal{H} + \mathcal{L}(\rho(u_\eta - D_n)) + \rho \cdot \mathcal{L}(D_n)),$$

$$C = (D_n - u_\eta) \cdot (\mathcal{H} + \mathcal{L}(D_n)) + \frac{1}{\rho} \mathcal{L}(P) - \mathcal{L}(E + 1/2(D_n - u_\eta)^2 + \frac{P}{\rho}),$$

$$\mathcal{E} = -\frac{P_{,\xi}}{\rho(1 - \eta\kappa_s)} + \frac{u_\eta \mathcal{H} - \mathcal{L}(u_\xi)}{u_\xi},$$

$$\mathcal{G} = \frac{\rho}{(1 - \eta\kappa_s)} (\kappa_s u_\eta + u_{\xi,\xi}),$$

$$\mathcal{H} = \frac{u_\xi}{(1 - \eta\kappa_s)} (D_{n;\xi} - \kappa_s u_\xi),$$

$$\mathcal{L}(\cdot) = \epsilon \frac{D}{D\tilde{t}} + \epsilon \frac{D\lambda^{(1)}}{D\tilde{t}} \frac{\partial}{\partial \lambda} + O(\epsilon^{2+\delta}),$$

# DSD - 4

---

- $D_n(\kappa)$  scalings in the limit  $(\eta_{rz} \kappa) = O(1)$

$$\tilde{t} = \epsilon^\nu t, \quad \tilde{\xi} = \epsilon^\sigma \xi, \quad \phi = \epsilon^{-\sigma} \tilde{\phi}$$

- with  $\kappa = \tilde{\phi}, \tilde{\xi} = O(1)$
- when  $\nu$  and  $\sigma$  are sufficiently large, time and transverse spatial variations are neglected to get the leading order, quasi-steady nozzle theory

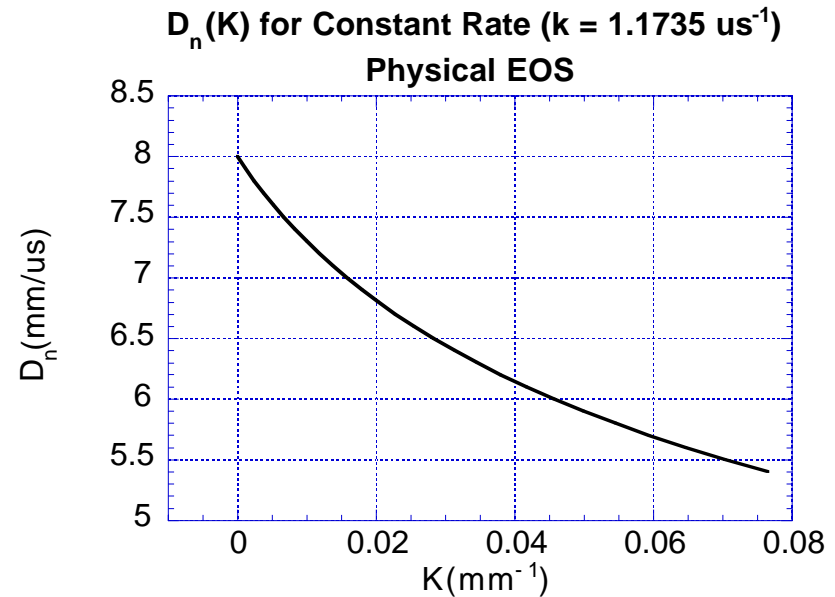
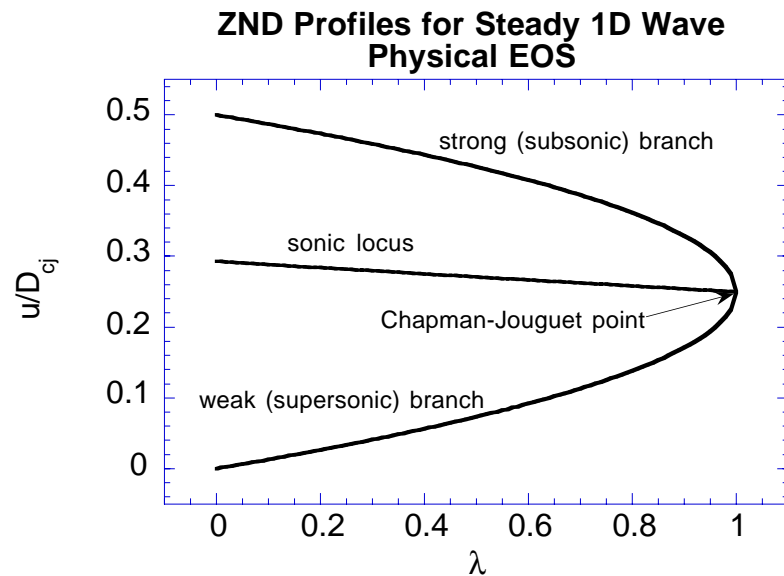
$$\left[ (D_n - u_\eta)^2 - c^2 \right] \frac{du_\eta}{d\lambda} = \frac{E_{,\lambda} (D_n - u_\eta)}{\rho E_{,P}} - \frac{c^2 u_\eta (D_n - u_\eta) \kappa}{R}$$

which with the Bernoulli equation,  $R$ , and the shock conditions defines a shooting problem for  $D_n(\kappa)$

- $D_n - \kappa$  theory

# DSD - 5

- $u_\eta$  vs  $\lambda$  phase plane



- eos and rate model  
 $\rho_0 = 2 \text{ gm/cc}$ ,  $\gamma = 3$ ,  
 $q = 4 \text{ mm}^2/\mu\text{s}^2$

$$R = 1.1735/\mu\text{s}, \quad 0 < \lambda < 1$$

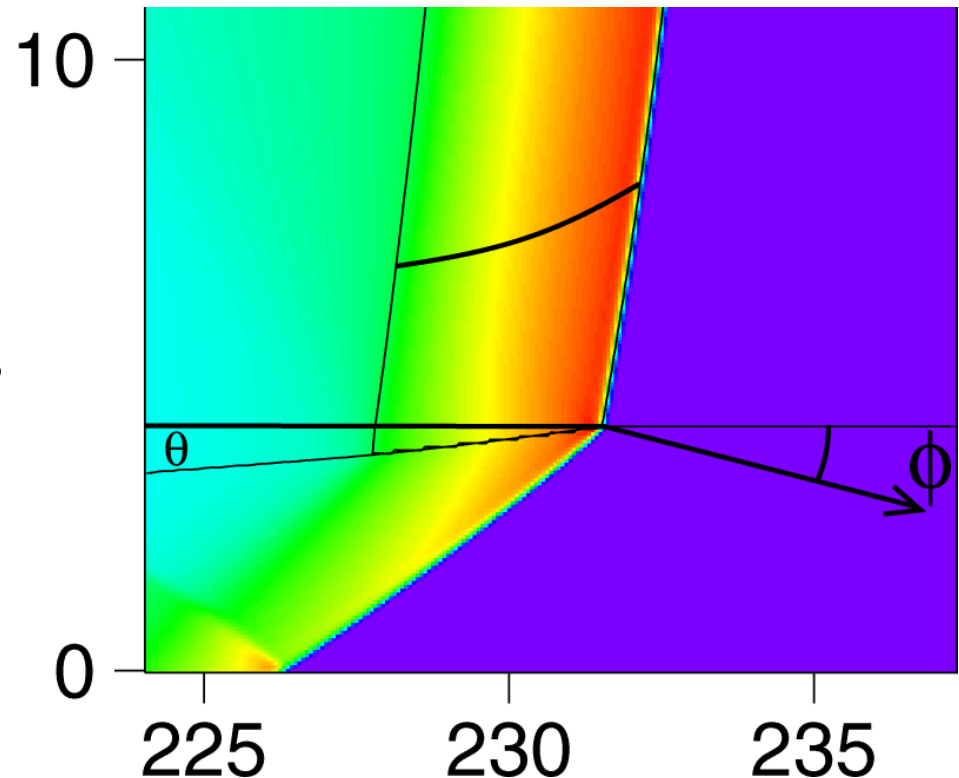
$$R = 0, \quad \lambda > 1$$

- the front propagation law is  $D_n(\kappa)$ . Parabolic PDE for front dynamics

$$\mathcal{L}(\phi) = -\frac{dD_n}{d\kappa} \frac{\partial^2 \phi}{\partial \xi^2}.$$

# $D_n(\kappa)$ Boundary Conditions - 1

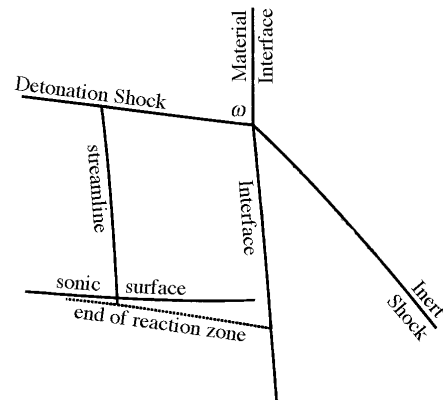
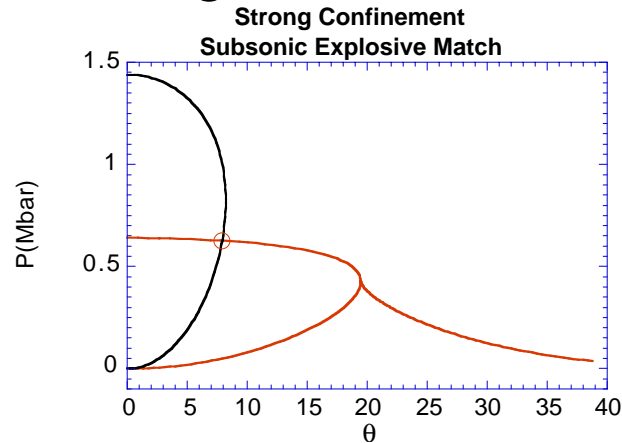
- nozzle ODEs apply only away from boundaries
- boundary layer exists near interfaces
  - governed by “steady” elliptic (hyperbolic) PDEs for subsonic (supersonic) flows
- $D_n(\kappa)$  front dynamics requires boundary condition on  $\phi$
- boundary layer solutions
  - shock polar analysis
  - solution of PDEs for small streamline deflection



# $D_n(\kappa)$ Boundary Conditions - 2

- shock polars

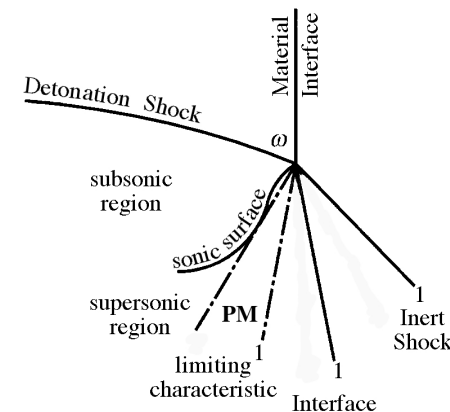
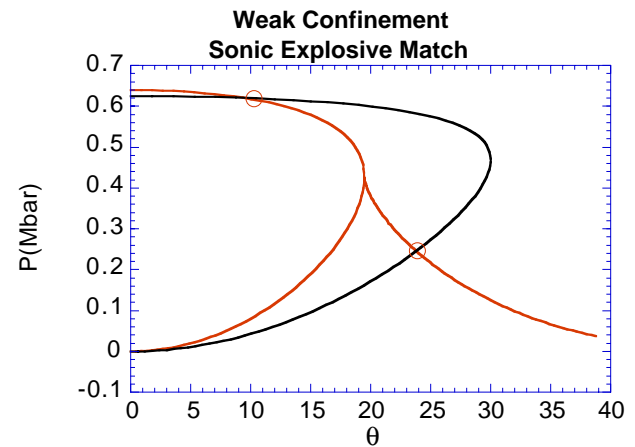
strong confinement



$$\phi_e = 8.25, \phi_{DSD} = 9.65$$

$$\omega = \pi/2 - \phi$$

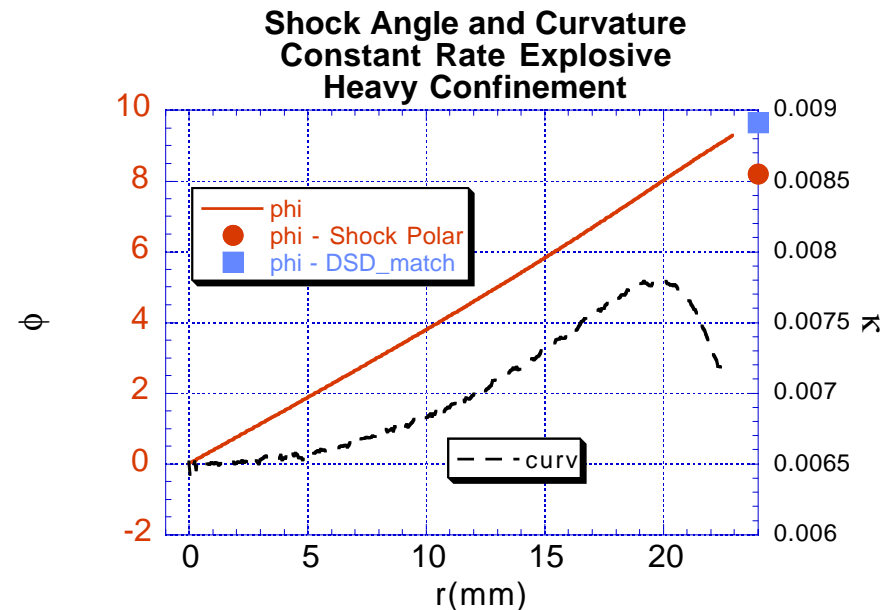
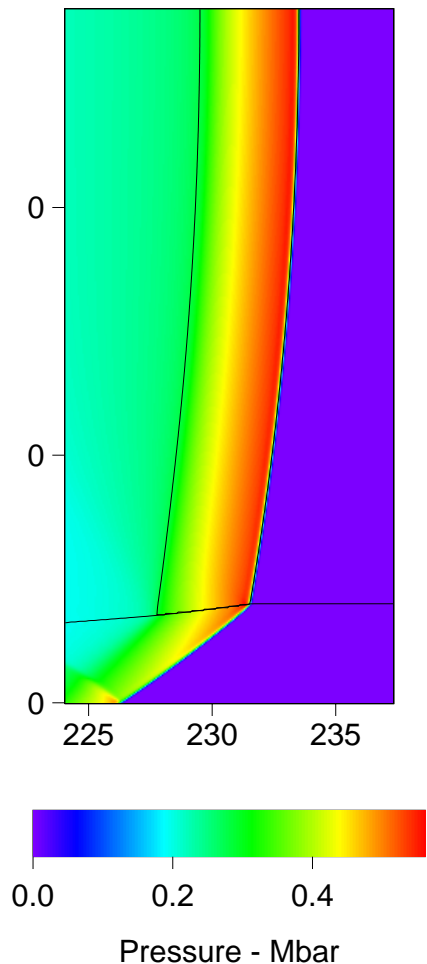
weak confinement



$$\phi_e = \phi_{DSD} = 35.3$$

# $D_n(\kappa)$ Boundary Conditions - 3

- direct numerical simulation  
-- strong confinement



- boundary layer-type analysis  
gives relation for transforming

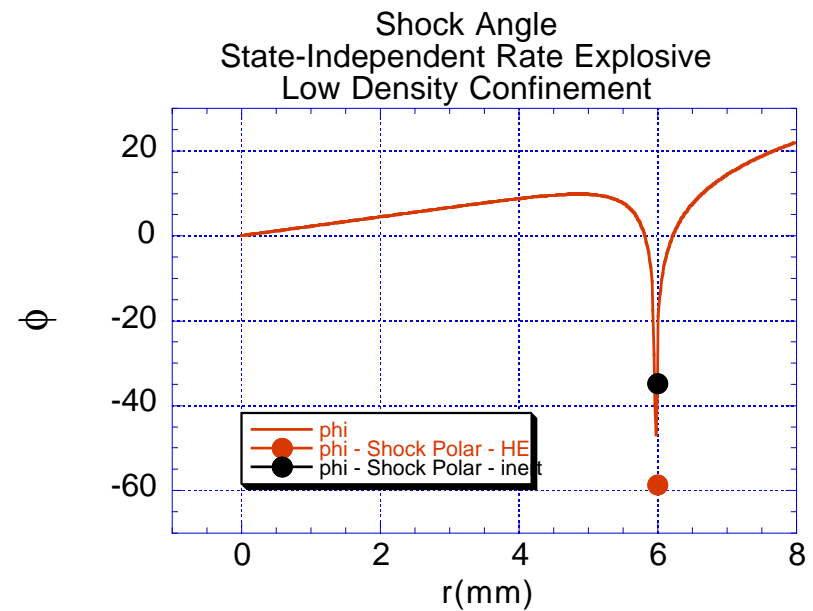
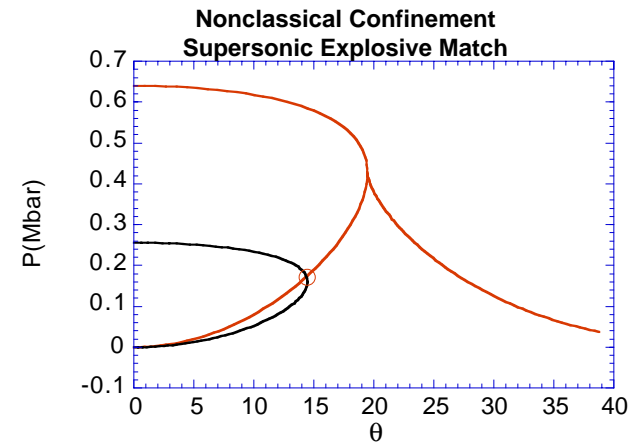
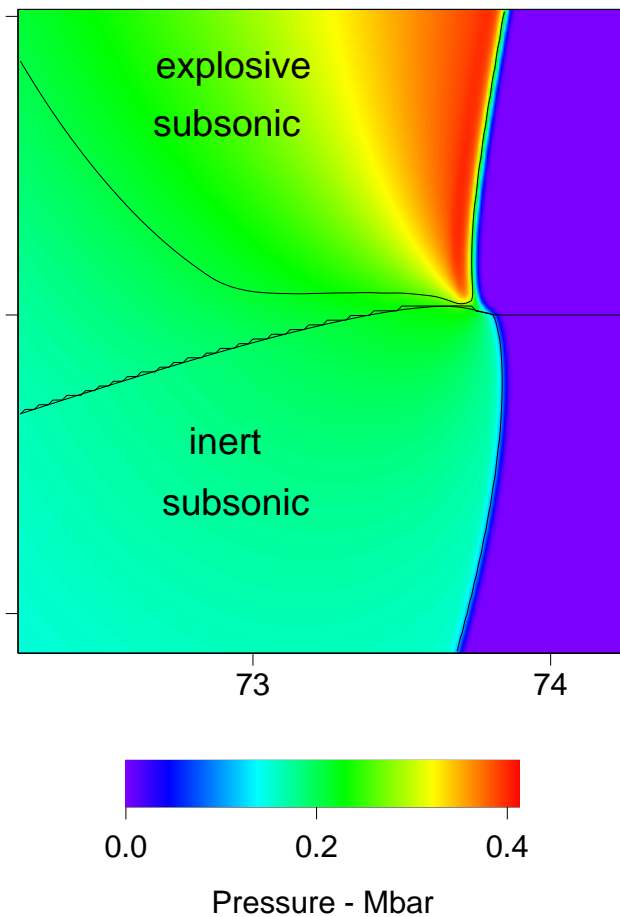
$\theta_e$  to  $\theta_{eDSD}$

$$\tan(\theta_{eDSD}) = L \tan(\theta_e)$$

$L = 1.155$ , constant rate HE

# $D_n(\kappa)$ Boundary Conditions - 4

- direct numerical simulation
  - nonclassical case, with inert “pulling” the explosive



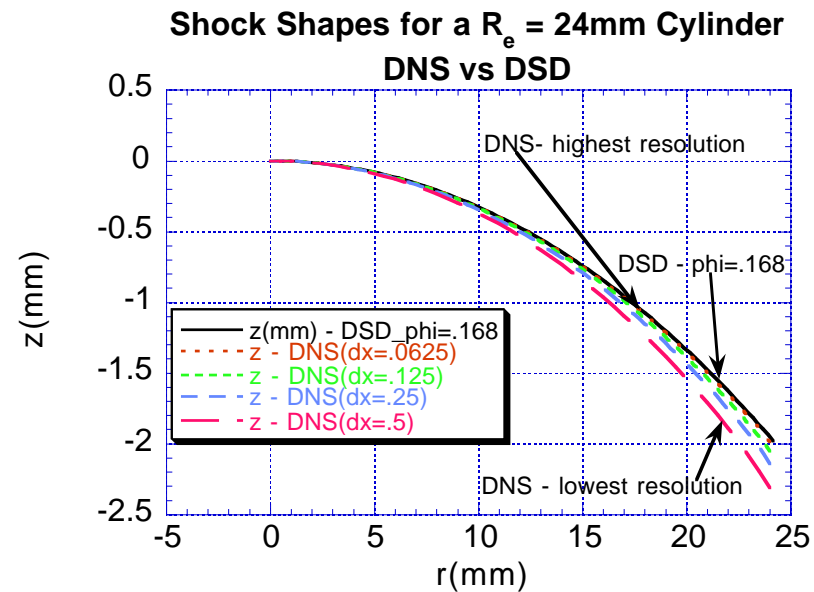
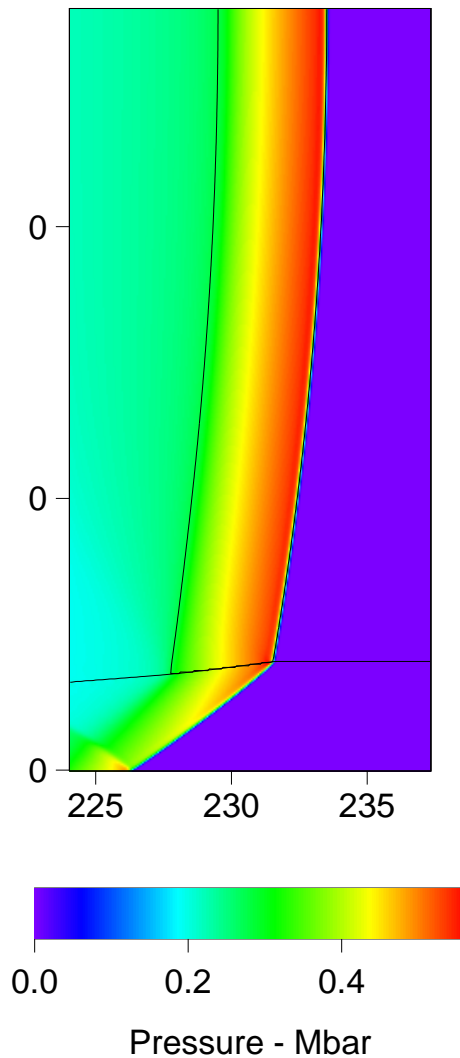
# $D_n(\kappa)$ Boundary Conditions - 5

---

- in summary, the DSD boundary algorithm for  $\omega$  is:
  - compute  $\omega_s$  for the sonic shock state
  - compute  $\omega$  using shock polars for the interface inert  
if  $\omega$  is larger than  $\omega_s$  call this  $\omega_c$   
modify  $\omega_c$  following the boundary layer analysis
  - measure the  $\omega$  of the front at the interface
    - when  $\omega < \omega_s$  then apply extrapolation,  $\vec{t}_s \cdot \vec{\nabla} \omega = 0$
    - when  $\omega > \omega_s$  then set  $\omega = \omega_c$  or  $\omega = \omega_s$ , which ever gives the lower match pressure

# $D_n(\kappa)$ Shock Shape Prediction

- comparison of a DSD and DNS calculated shock



# DSD Front-Flow Coupling

---

## Design Principles

- the dynamics of DSD fronts is decoupled from the following flow
- the following flow depends crucially on the front motion
  - the proper detonation energy must be delivered to the flow
  - the detonation exit state (pressure, density, velocities) seeded into the following flow must be correct
  - mass, momentum and energy conservation must be maintained
- small inconsistencies between the following flow and the front motion must not be permitted to influence the front motion
  - the DSD front must act as a trigger wave that is the first signal propagated into the unburnt explosive
- DSD reaction zone

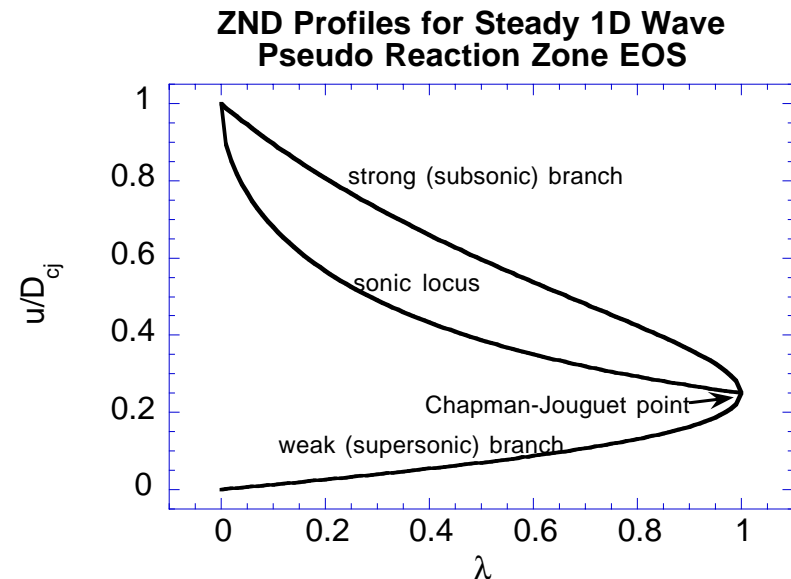
# DSD Reaction Zone - 1

- equation of state for the DSD reaction zone

$$\underline{E(P/\lambda, \rho)}, \quad E = \frac{P\rho}{(\gamma - 1)\lambda}, \quad \text{with } E_0 = \frac{D_{CJ}^2}{2(\gamma^2 - 1)}$$

$$\frac{\rho}{P} \left( \frac{\partial P}{\partial \rho} \right)_S = 1 + (\gamma - 1)\lambda$$

$$c^2 = (1 + (\gamma - 1)\lambda) \frac{P}{\rho}$$



- reaction rate for the DSD reaction zone

$$R = \frac{D_t}{\eta_{prz}}, \quad 0 \leq \lambda \leq 1$$

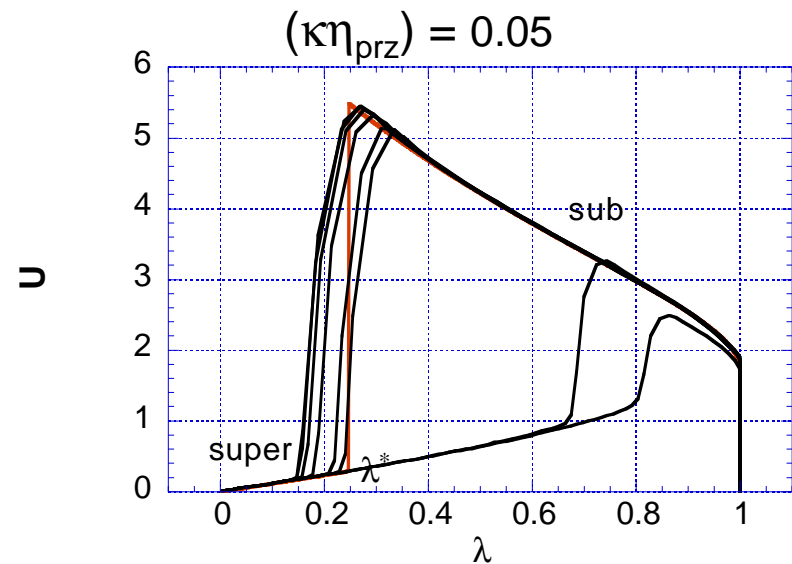
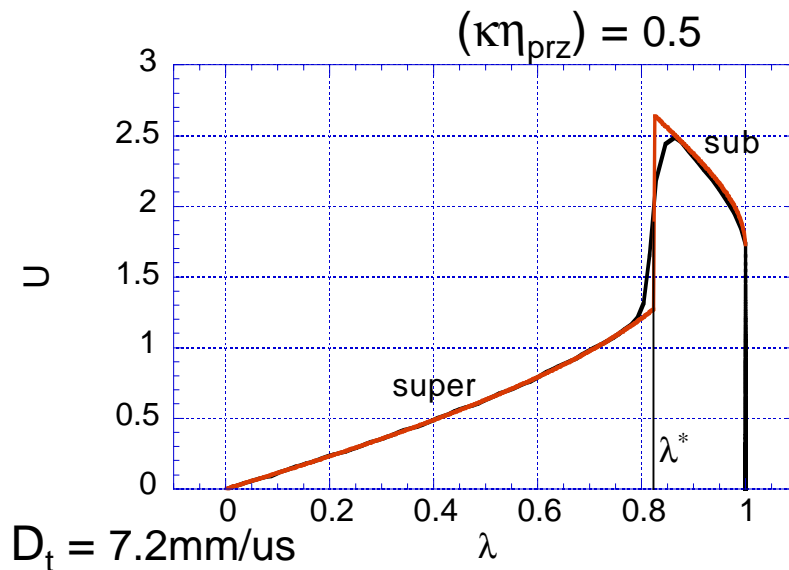
$$R = 0, \quad \lambda \geq 1$$

# DSD Reaction Zone - 2

- analysis of the reaction-zone structure problem for the DSD reaction zone ( $D_t$ ,  $\kappa$  and  $\eta_{prz}$  specified)

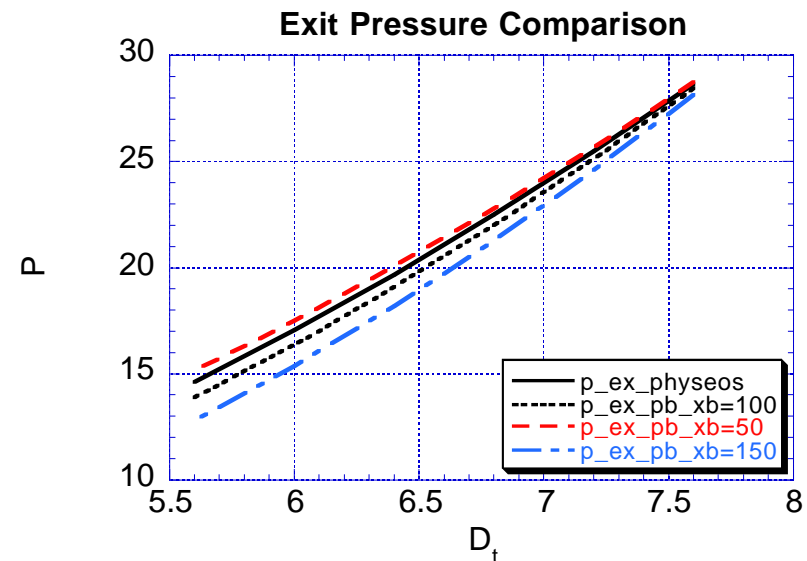
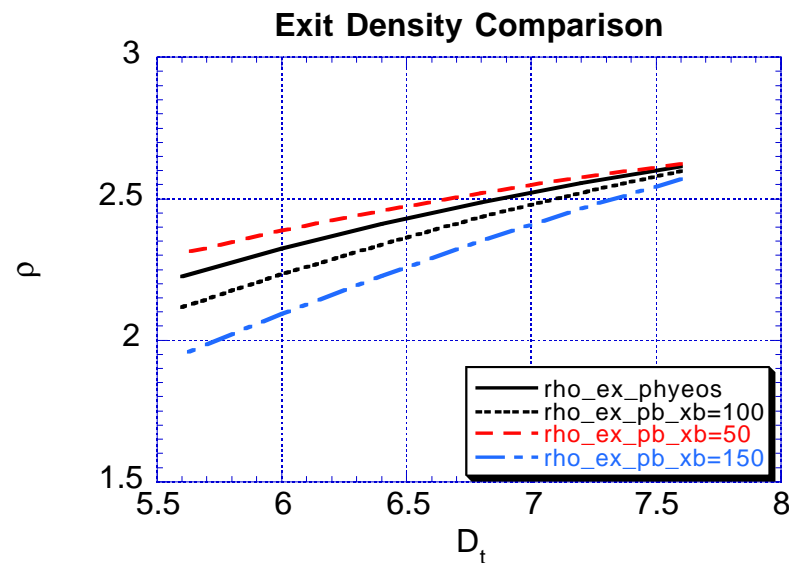
$$\left[ (D_t - u_\eta)^2 - c^2 \right] \frac{du_\eta}{d\lambda} = \frac{(D_t - u_\eta)c^2}{(1 + (\gamma - 1)\lambda)\lambda} - \frac{c^2 u_\eta (D_t - u_\eta) \kappa}{R},$$

- trigger supported reaction zone structures
  - the ratio  $(\kappa\eta_{prz})$  controls the profile (the location of the internal shock,  $\lambda^*$ )



# DSD Reaction Zone - 3

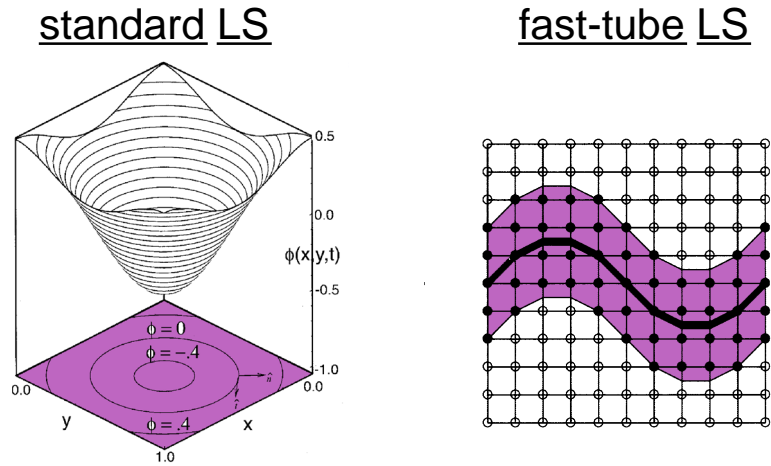
- exit state controlled principally by  $D_t$  and secondarily by  $\eta_{prz}$ . The exit value of  $u_\eta$  is exact



- exit state from the physical model and the DSD reaction zone can be made identical

# Implementation: Front Algorithm

- fast-tube level-set front propagator
  - complex topologies
  - efficient



high order smoothness needed in level-set field for accurate solutions

LS PDE

$$\frac{\partial \phi}{\partial t} + D_n(\kappa) = 0,$$

redistance PDE

$$\frac{\partial \phi}{\partial \tau} = S(\phi) \cdot [1 - |\vec{\nabla} \phi|], \quad S(\phi) = \frac{\phi}{\sqrt{\epsilon^2 + \phi^2}},$$

fast-tube algorithm is O(N) faster. Huygens problem scales like O(N<sup>2</sup>)

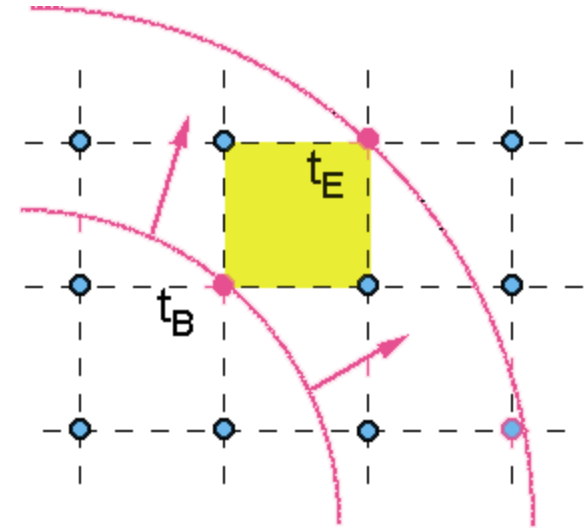
<u>N x N</u>	<u>time</u>	<u>N<sup>x</sup></u>
150x150	~10 s	
300x300	~50 s	2.3
600x600	~335 s	2.7
1200x1200	~2350 s	2.8

# Implementation: Reaction & Linking

- DSD uses a pseudo reaction zone  
--  $\lambda$  is prescribed function of time

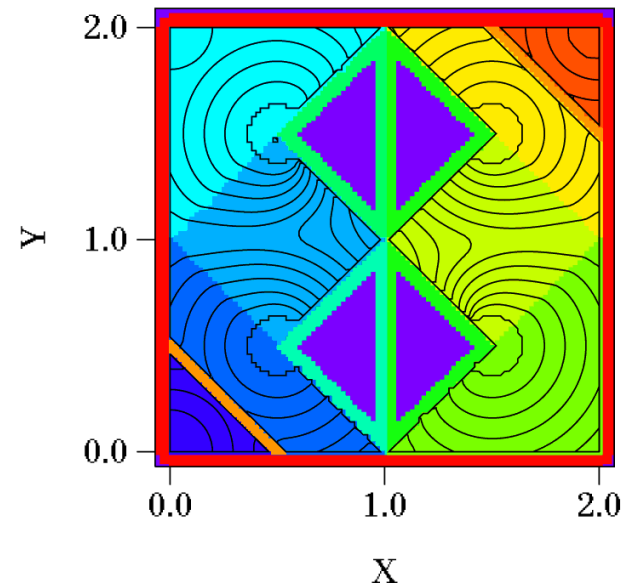
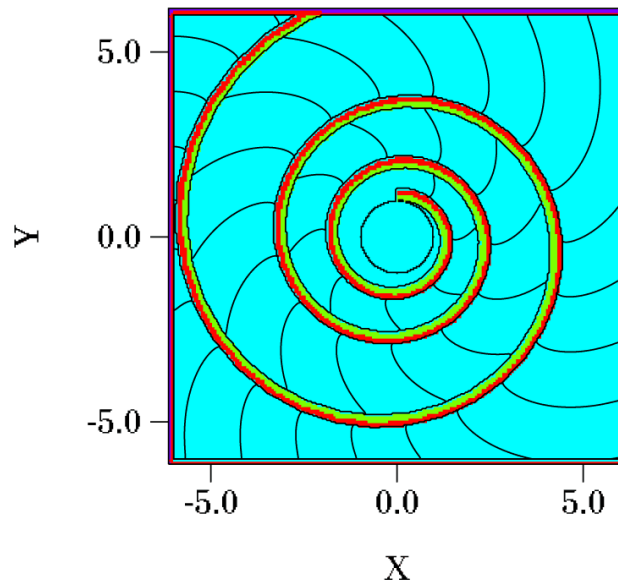
$$\lambda = \min \left[ 1.0, \max \left( 0.0, \left( \frac{t - t_B}{t_E - t_B} \right) \frac{1}{b_{fc}} \right) \right],$$

$$b_{fc} = \max \left( 1.0, \frac{n_{prz}}{D_t \cdot (t_E - t_B)} \right)$$



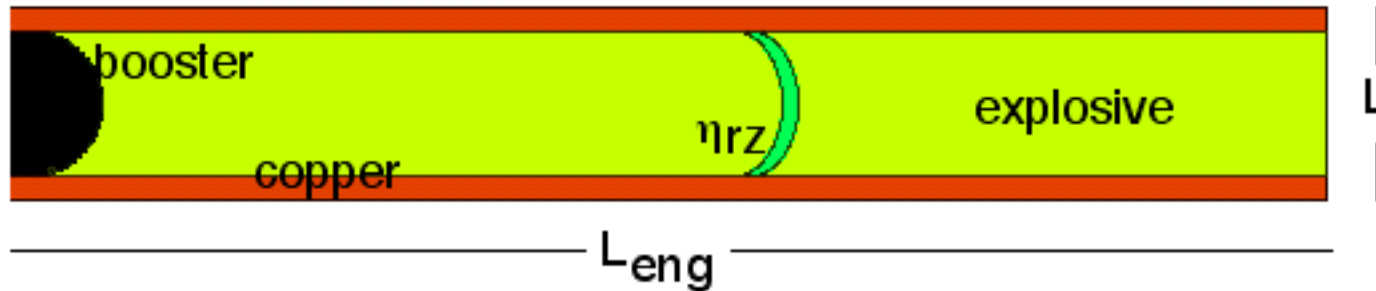
# Implementation: Examples

- features:
  - multiple contacting or isolated explosive regions
  - detonation across explosive/explosive boundaries
  - interfaces with multiple inerts
  - complex  $D_n(\kappa)$  forms
  - complex explosive shapes
  - many, nonsimultaneous detonation ignition points



# Model Explosive: DSD vs DNS - 1

- direct comparisons on the the detonation cylinder for the model constant rate explosive copper confinement

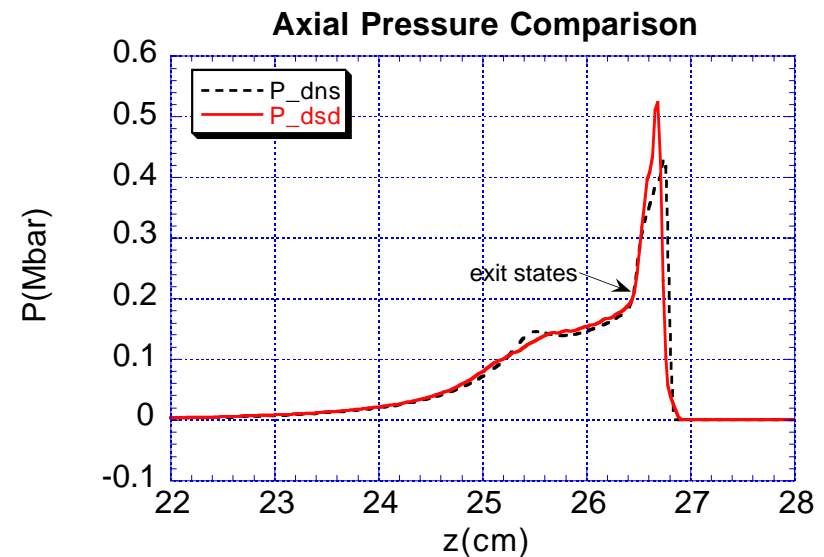
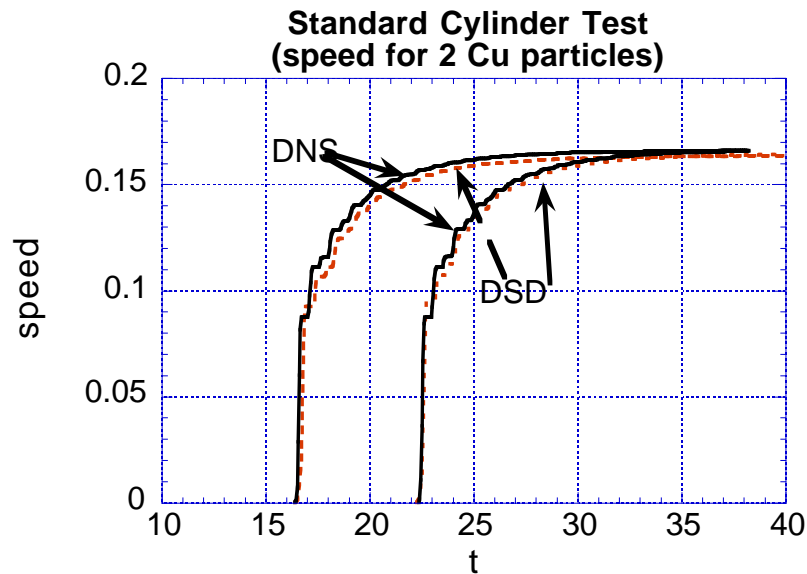
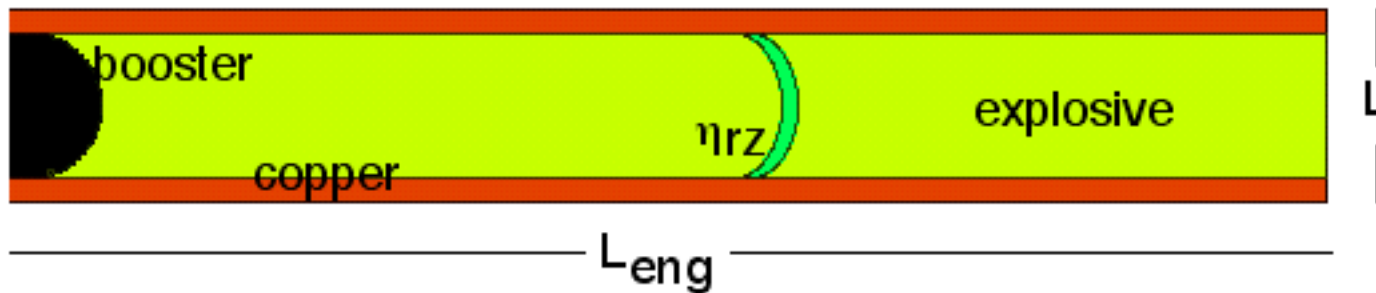


- DSD uses the  $D_n(\kappa)$  relation shown,  $\omega_s = 0.9553$ ,  $\omega_c = 1.4386$  and the physical reaction-zone length of  $\eta_{rz} = 4$  mm ( $D_0 - DSD = 6.805$  mm/ $\mu$ s -- exact)

<u>resolution</u>	<u><math>D_0 - DNS</math></u>	<u><math>D_0 - DSD</math></u>
80x310 (1.0 mm)		6.729 mm/ $\mu$ s
160x620 (0.5 mm)	6.769 mm/ $\mu$ s	6.807 mm/ $\mu$ s
320x1240 (0.25 mm)	6.739 mm/ $\mu$ s	6.792 mm/ $\mu$ s
640x2480 (0.125 mm)		6.802 mm/ $\mu$ s

# Model Explosive: DSD vs DNS - 2

- comparison of axial pressure and tangential acceleration of copper liner



# Calibration to a Solid Explosive

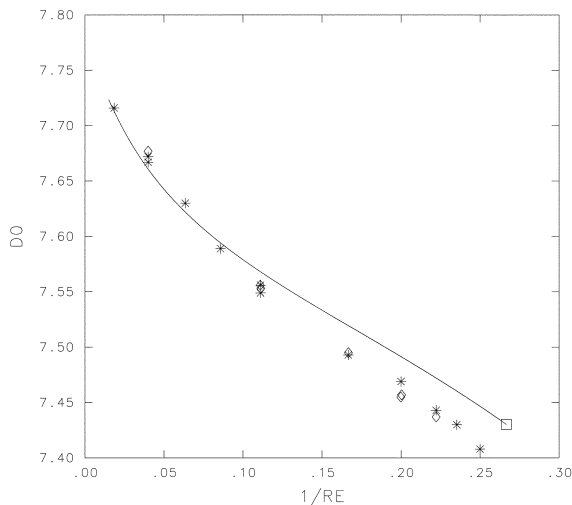
- direct calibration of  $D_n(\kappa)$  to experimental wave shape and velocity data gathered on explosive cylinders of various radii and colliding detonation

- assume a unique  $D_n(\kappa)$  exists

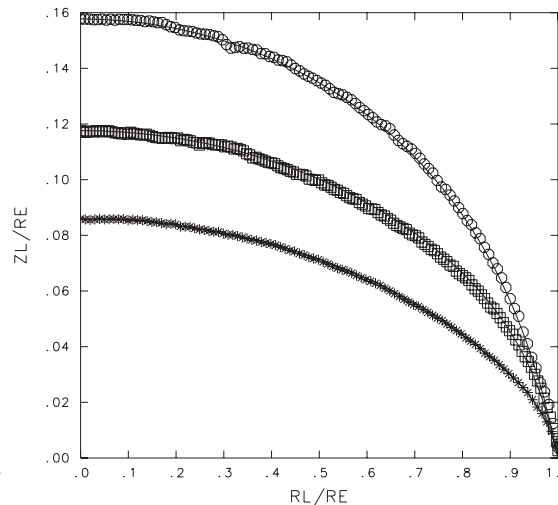
$$\frac{D_n}{D_{CJ}} = 1 - B \cdot \kappa \cdot \frac{(1 + C_2 \cdot \kappa^{e_2} + C_3 \cdot \kappa^{e_3})}{(1 + C_4 \cdot \kappa^{e_4} + C_5 \cdot \kappa^{e_5})}$$

- Levenberg-Marquardt least-squares fit

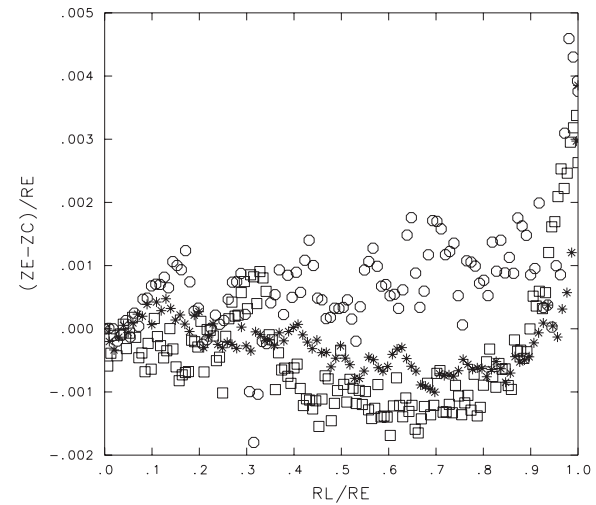
DIAMETER-EFFECT CURVE



SHOCK LOCI

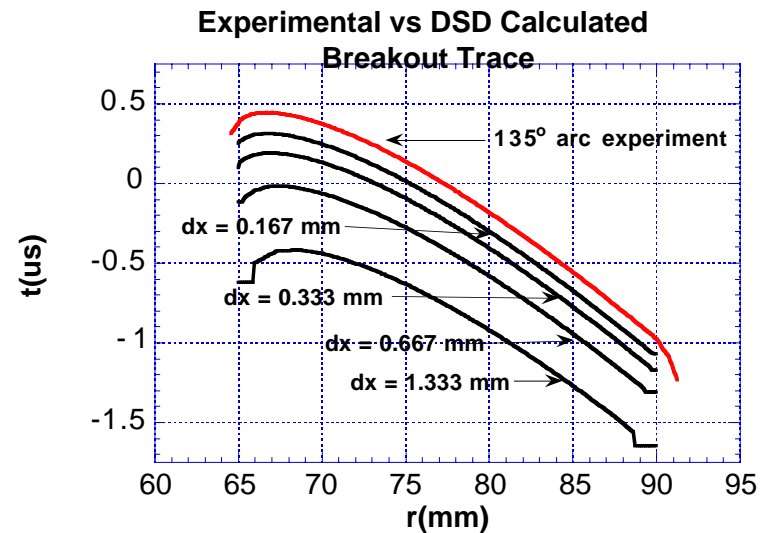
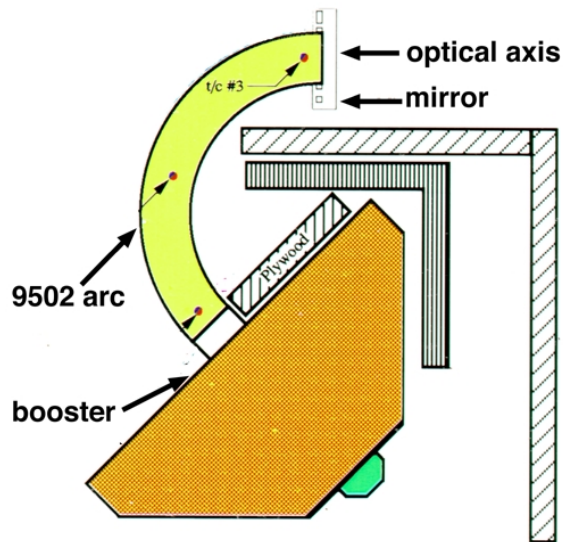
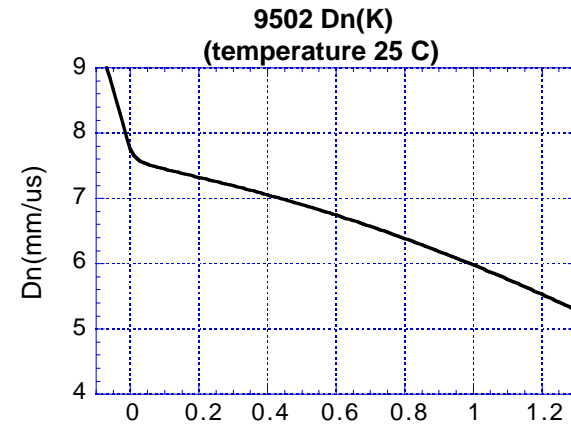


SHOCK RESIDUALS



# Predictions using $D_n(\kappa)$ Law

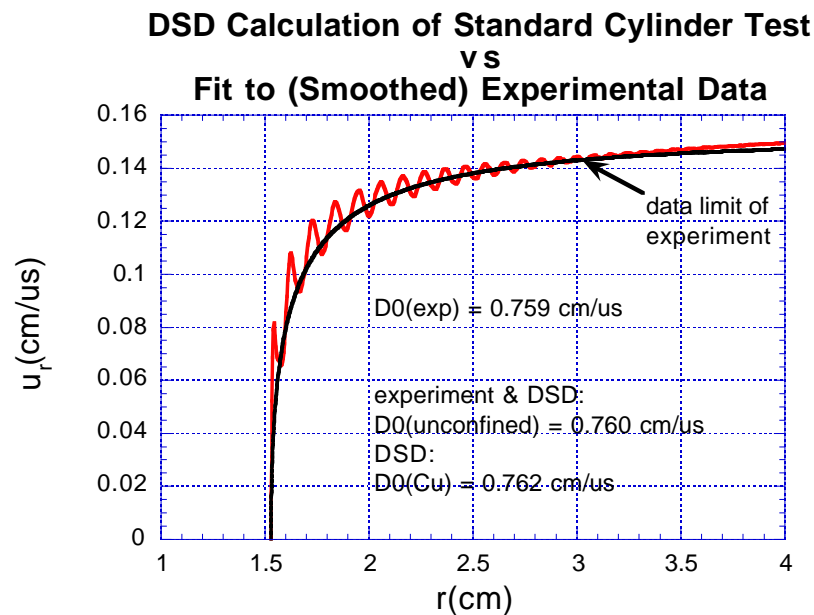
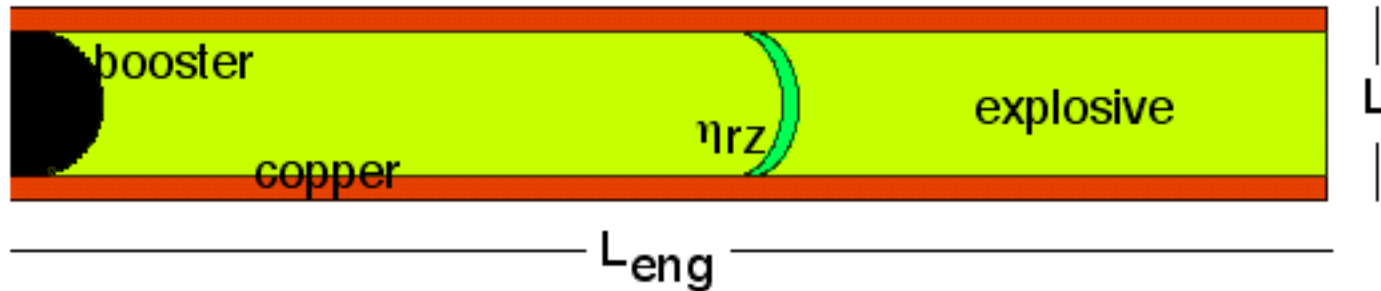
- calibration results,  
 $D_{CJ} = 7.764 \text{ mm}/\mu\text{s}$   
 $\omega_s = 0.8674$
- prediction on planar arc



<i>phase velocity</i>	<i>exp</i>	<i>DSD</i>
$D0_{in}(\text{mm}/\mu\text{s})$	7.188	7.198
$D0_{out}(\text{mm}/\mu\text{s})$	9.953	9.961

# Predictions using DSD

- comparison with data on cylinder test for a solid explosive



# Higher Order DSD Theory - 1

- simple arguments indicate time dependence may be important

$$\mathcal{L}(D_n) = -(D_0 \sin(\phi))^2 \kappa$$

- general scalings, with  $\kappa = O(\epsilon)$

$$\tilde{t} = \epsilon^\nu, \quad \tilde{\xi} = \epsilon^\sigma \xi, \quad \phi = \epsilon^{1-\sigma} \tilde{\phi},$$

$$\mathcal{D} = \epsilon^\beta \tilde{\mathcal{D}} = (D_n - D_{CJ})/D_{CJ},$$

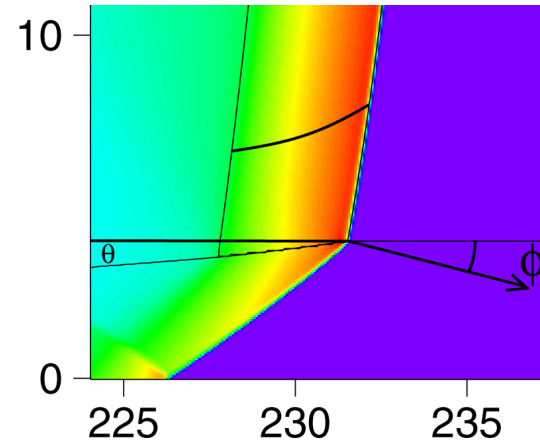
- scaled result

$$\epsilon^{\nu+\beta} D_{CJ} \tilde{\mathcal{L}}(\tilde{\mathcal{D}}) = -\epsilon D_0^2 \left( \sin(\epsilon^{1-\sigma} \tilde{\phi}) \right)^2 \frac{\partial \tilde{\phi}}{\partial \tilde{\xi}},$$

- DSD scalings, based on  $(D_n/D_{CJ} - 1)$  and  $\kappa$  being  $O(\epsilon)$

$$\tilde{t} = \epsilon t, \quad \tilde{\xi} = \epsilon^{1/2} \xi, \quad \phi = \epsilon^{1/2} \tilde{\phi}, \quad \mathcal{D} = \epsilon \tilde{\mathcal{D}} = (D_n - D_{CJ})/D_{CJ}$$

$$\kappa = O(\epsilon), \quad \mathcal{L}(D_n) = O(\epsilon^2)$$



# Higher Order DSD Theory - 2

---

- consider  $\kappa$  as a dependent variable with the expansion

$$\kappa(\mathcal{D}) = \epsilon \kappa^{(1)} + \epsilon^2 \kappa^{(2)} + \dots$$

- seek a formal expansion of  $Y = (\rho, u_\eta, P)^T$  of the form

$$Y = Y^{(0)} + \epsilon Y^{(1)} + \epsilon^2 Y^{(2)} + \dots$$

$$u_\xi = \epsilon^{3/2} u_\xi^{3/2} + \dots \quad \lambda = \lambda^{(0)} + \epsilon \lambda^{(1)} + \dots$$

- where we can solve for  $\lambda^{(1)}$  knowing only  $R^{(0)}$

$$\lambda^{(1)} = \tilde{\mathcal{D}} \tilde{L}(\eta) = \tilde{\mathcal{D}} L(\lambda^{(0)}) = \tilde{\mathcal{D}} L(\lambda),$$

- to get an explicit expression for the time derivative in our transformed coordinates

$$\tilde{\mathcal{L}}(\ ) = \epsilon \frac{D}{D\tilde{t}} + \epsilon \frac{D\lambda^{(1)}}{D\tilde{t}} \frac{\partial}{\partial \lambda} + O(\epsilon^{2+\delta}),$$

- where  $\frac{D}{Dt} = \frac{\partial}{\partial t} + D_n \vec{n} \cdot \vec{\nabla}$

# Higher Order DSD Theory - 3

---

- using the intrinsic coordinate equations, at  $O(\varepsilon)$  we get

$$\bar{M} \cdot \bar{Y}^{(1)} = \bar{N}^{(1)},$$

- a solvability condition involving  $\bar{M}^{-1}$  returns the condition

$$-\frac{D_{cj}\kappa^{(1)}}{k} = \left(\frac{\gamma+1}{\sqrt{2}\gamma}\right)^2 \left(\frac{h}{2^h-1}\right) \tilde{\mathcal{D}} \equiv \frac{\tilde{\mathcal{D}}}{\alpha},$$

- at  $O(\varepsilon^{3/2})$ , we get

$$u_{\xi,\lambda}^{(3/2)} = -\frac{1}{R^{(0)}\rho^{(0)}} P_{,\tilde{\xi}}^{(1)} + \frac{D_{cj}u_{\eta}^{(0)}}{R^{(0)}} \tilde{\mathcal{D}}_{,\tilde{\xi}},$$

- and finally at  $O(\varepsilon^2)$ , we get

$$\bar{M} \cdot \bar{Y}^{(2)} = \bar{N}^{(2)}.$$

- which returns via a solvability condition,  $\kappa^{(2)}$

$$\kappa^{(2)} \left( \tilde{\mathcal{D}}^2, \frac{D\tilde{\mathcal{D}}}{D\tilde{t}}, \frac{\partial^2 \tilde{\mathcal{D}}}{\partial \tilde{\xi}^2} \right).$$

- combining and suppressing  $\varepsilon$ -dependence gives

$$\bar{\kappa} = \mathcal{F}(\mathcal{D}) - A \frac{D\mathcal{D}}{D\bar{t}} + B \frac{\partial^2 \mathcal{D}}{\partial \bar{\xi}^2} \quad \bar{\kappa} \equiv \frac{\kappa_s D_{cj}}{k}, \bar{t} \equiv kt, \bar{\xi} \equiv \frac{k}{D_{cj}} \xi,$$

# Higher Order DSD Theory - 4

---

- replacing series by “likely” closed form expressions

$$1 - 2\mathcal{D} + 3\mathcal{D}^2 + \dots = (1 + \mathcal{D})^{-2},$$

$$-\mathcal{D} - m\mathcal{D}^2 + \dots = -\mathcal{D}(1 + \mathcal{D})^m,$$

- finally yields a DSD propagation law through  $O(\varepsilon^2)$

$$(1 + \mathcal{D})^{1-2n} \bar{\kappa} = -\frac{\mathcal{D}(1 + \mathcal{D})^{1-2n-\tilde{f}_2}}{\alpha} + B \frac{\partial^2 \mathcal{D}}{\partial \xi^2}$$
$$- \left( A + \frac{3(\gamma + 1)}{2\gamma} \left( (1 + \mathcal{D})^{-1-2n} - 1 \right) \right) \frac{D\mathcal{D}}{Dt}.$$

- like  $D_n(\kappa)$ , this propagation law has parabolic dynamics
- both the shape (say as  $\phi$ ) and  $D_n$  must be given initially
- a boundary condition on  $(\phi + b\mathcal{D}_{,\xi})$  must be given
- we use this model to predict steady detonation in cylinders
- we specify  $\phi$  at the edge and  $\kappa$  on the axis

# Higher Order DSD Theory - 5

---

- we examine the following two cases and compare results with high-resolution DNS

case-1

$$n = 0, \quad \mu = 0.5, \quad k = 2.5147 \mu s^{-1}$$

$$\tilde{f}_2 = 2.6581, \quad A = 1.332, \quad B = 0.2024$$

case-2

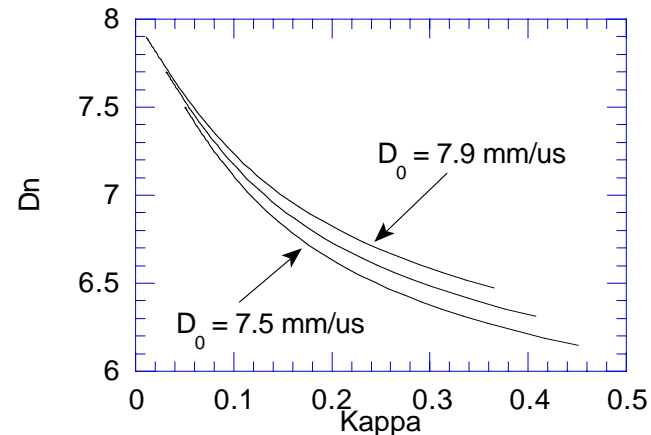
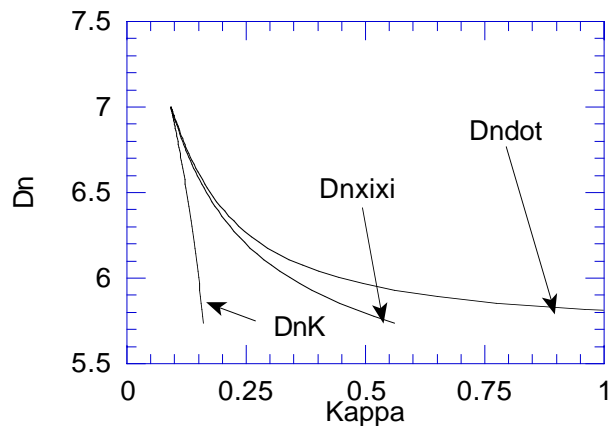
$$n = 2, \quad \mu = 0.5, \quad k = 1.2936 \mu s^{-1}$$

$$\tilde{f}_2 = -1.3636, \quad A = 3.821, \quad B = 0.2148$$

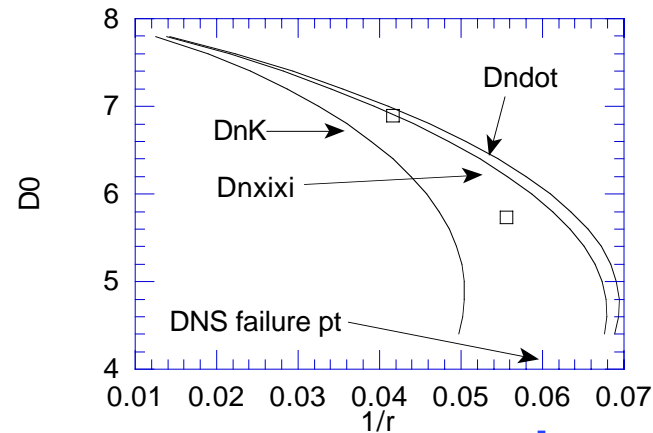
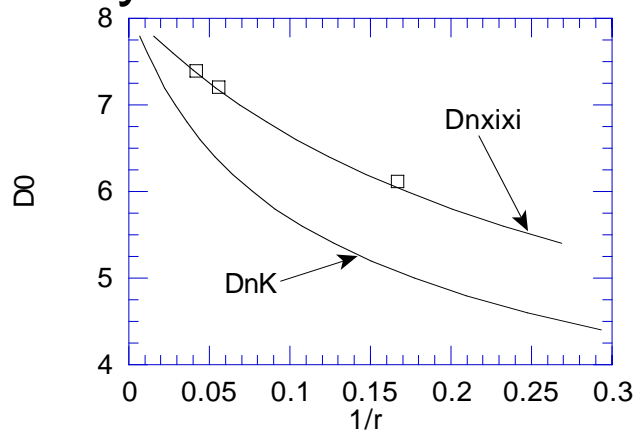
- we consider 3 limits, the full model (Dnxixi), Dndot and DnK, for their predictions
- we stress the model by making  $\phi_e$  large (unconfined) and  $D_0$  far from  $D_{CJ}$

# Higher Order DSD Theory - 6

- comparison of  $D_n$  vs  $\kappa$  along a shock for various models and conditions



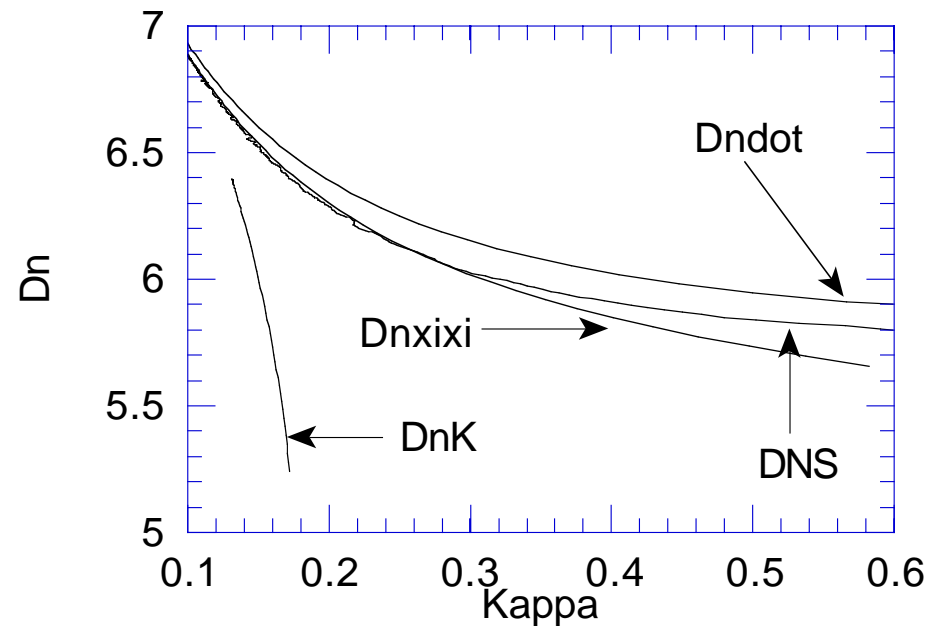
- comparison of DSD with DNS for detonation phase velocity curves



# Higher Order DSD Theory - 7

---

- higher order theory gives good prediction of very sensitive variables on difficult case

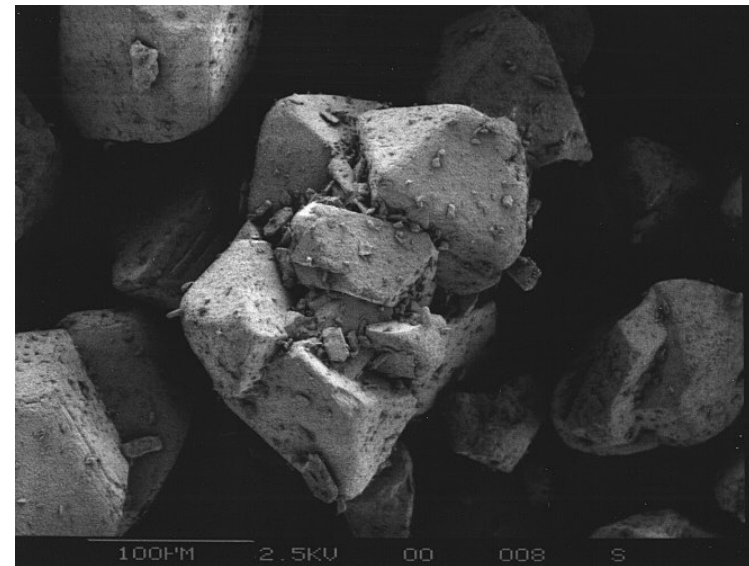


# $D_n(\kappa, \dots)$ Law vs Euler Models

---

- real heterogeneous solid explosives are complex
- grain size can be of the order of the reaction length
- competition between second order effects determines 2D propagation
- empirical reaction rates are not “physically” correct at level of second order effects
- $D_n(\kappa, \dots)$  laws obtained directly from experiment with support from theory

HMX grains



# Summary

---

- an overview of the elements of the DSD model
- elements of a DSD implementation
- examples of how DSD compares with DNS
- ability to predict results of physical experiments
- higher order theory
- argument on why subscale, calibrated models are needed to get highly accurate predictions of detonation propagation